Development of *In Situ* Blends of Poly(*p*-oxybenzoate-*co*-*p*-phenyleneisophthalate) with Other Thermotropic Liquid Crystalline Polymers

BALARAM GUPTA, GORDON CALUNDANN, LARRY F. CHARBONNEAU, H. CLAY LINSTID, JAMES P. SHEPHERD, and LINDA C. SAWYER

Hoechst Celanese Advanced Technology Group, Robert L. Mitchell Technical Center, 86 Morris Avenue, Summit, New Jersey 07901

SYNOPSIS

A new *in situ* polymerization method is discussed wherein monomers of the major component are polymerized in the presence of a preformed thermotropic liquid crystalline polymer (LCP). Poly(*p*-oxybenzoate-*co*-*p*-phenyleneisophthalate) (HIQ) was chosen for this study. HIQ is well known to have a narrow process window and to be difficult to process reproducibly, both drawbacks for a commercial product. An *in situ* polymerization of the HIQ monomers in the presence of a fully polymerized LCP, such as poly(4-oxybenzoate-*co*-6-oxy-2-naphthoate) (CO) results in the "CO–HIQ" *in situ* blend. The *in situ* blend exhibited reduced biphasic morphology and was more homogeneous than was HIQ. The glass fiber-filled CO–HIQ resin also featured improved melt flow and more reproducible mechanical properties than those of HIQ. The *in situ* blends were characterized by optical microscopy, ^{1}H-NMR, and melt rheology. The effect of the LCP level on the morphology of the *in situ* blend is discussed. © 1994 John Wiley & Sons, Inc.

INTRODUCTION

The copolyester, poly(*p*-oxybenzoate-*co*-*p*-phenyleneisophthalate) (HIQ) was originally synthesized by Cottis et al.[1] HIQ is a copolyester of *para*-hydroxybenzoic acid (HBA), isophthalic acid (IA), and hydroquinone (HQ). The 4-oxybenzoate segments, resulting from HBA, impart nematogenicity, causing the copolyester to be liquid crystalline in the temperature range of 280–400°C. At the same time, the IA and HQ form 1,4-phenyleneisophthalate segments that are known to form a crystalline structure similar to that of a flexible chain polymer such as poly(ethylene terephthalate).[2-3] Thus, when the composition of HIQ contains an equal level of these two ester linkages, it exhibits biphasic morphology, coexistent liquid crystalline, and crystalline phases. A particular composition of interest is HIQ at HBA/IA/HQ 35/32.5/32.5 (HIQ35), which has almost an equimolar ratio of both ester linkages and, thus, features pronounced biphasic morphology. It should be noted that both homopolymers of HBA and IA/HQ melt at higher than 400°C and, thus, are intractable. Also, HIQs with greater than 50% HBA or less than 25% HBA have melting points at or above 400°C and, thus, cannot be melt-processed.[2,4] Studies within Hoechst Celanese and by others[3] concluded that due to the biphasic nature of HIQ it is extremely difficult to obtain reproducible results from melt polymerization and subsequent melt processing.[4]

In recent years, several workers attempted to modify HIQ to suppress the biphasic nature and to take advantage of its liquid crystalline properties and low cost. The most striking example is from MacDonald and Ryan,[5] who were successful in modifying the morphology of HIQ by including an additional component: small amounts of 6-hydroxy-2-naphthoic acid (HNA). Their composition was made by a novel dispersion polymerization that exhibits uniform morphology and is claimed to have superior properties. Siemionko[6] disclosed compo-

Journal of Applied Polymer Science, Vol. 53, 575–586 (1994)
 CCC 0021-8995/94/050575-12

sitions of HIQ containing HNA in the 2.5–15 mol % range.

Cottis et al.[1] also reported HIQ compositions containing terephthalic acid (TA) as a fourth monomer, and, more recently, Layton et al.[7] obtained patents in Europe, Canada, and the United States on similar compositions containing TA as the additional monomer. These compositions overcome the shortcomings of low impact strength and low heat-deflection temperatures (HDTs) of HIQ, but have very high melting temperatures: 350–370°C.

Although the *in situ* technology reported here is novel for the synthesis of liquid crystalline polymers (LCPs), similar work has been reported for the synthesis of other polymers. For example, Matzner and Papuga[8] described compositions prepared by *in situ* polymerization of LCPs in the presence of fully polymerized thermoplastic polymers. These compositions have improved properties, in comparison to physical blends of the same compositions. The thermoplastic polymers used were poly(aryl ether ketone) (PEEK), poly(aryl ether) (PPO), and poly(aryl ether sulfone) (PAES). The LCPs made in the presence of these thermoplastics were CO (HBA/HNA), compositions containing 4,4′-biphenol (BP) (e.g., HBA/IA/TA/BP), phenylhydroquinone (PhHQ) and 2,6-naphthalene dicarboxylic acid (NDA) (e.g., TA/PhHQ/NDA), and poly(HBA). Sugimoto and Hanabata[9] reported the synthesis of variants by *in situ* polymerization of LCP monomers in the presence of fully polymerized thermoplastic polymers such as poly(ethylene terephthalate), polyphenylene sulfide, polyarylsulfones, and polyarylates. Ginnings[10] also described a process for preparing a polymer blend composition by melt blending an LCP with poly(ethylene terephthalate) prepolymer and, subsequently, solid-state polymerizing the blend. There are also innumerable reports claiming LCPs as process aids in a variety of physical blends.[11]

In the present study, we found that *in situ* polymerization of HIQ monomers in the presence of a small amount of fully polymerized LCP results in a considerable reduction of the biphasic nature of HIQ. Various LCPs were found to give similar results; however, in this article, we present the results of our work on the *in situ* polymerization of HIQ monomers in the presence of poly(4-oxybenzoate-*co*-6-oxy-2-naphthoate) (CO).[12]

EXPERIMENTAL

Materials

All materials used in this work were high-purity polymer grade and commercially available.

Thermal Analysis

Thermal analyses of the blends were performed on a Perkin-Elmer 7700 thermal analysis system. In all runs, the samples, sealed in aluminum pans, were heated or cooled at a rate of 20°C/min under nitrogen atmosphere. The DSC curves obtained from the second heating run were taken for the analysis.

Light Microscopy

Samples were prepared for microscopic analysis by thin sectioning using a glass knife microtome. The sections were examined by polarized light microscopy to observe morphological behavior at elevated temperatures. The thin sections of the polymer samples were held between quartz coverslips and heated at 20°C/min to a maximum temperature of 420°C followed by rapid quenching. The results were videotaped and micrographs were obtained from the videotape at four different temperatures: (A) room temperature, (B) 285°C, (C) 345°C, and (D) 395°C.

^{1}H-NMR Measurements

^{1}H-NMR spectra were recorded at 80°C using an external DMSO-d_6 lock on a Varian XL-200 NMR spectrometer operating at 200 MHz for protons. The spectra were recorded on polymer samples dissolved at about 1.3 wt % in pentafluorophenol-*d* (PFP-*d*).

Rheology

Melt viscosity measurements were made using a Kayeness melt rheometer Model 2052 with a Hastelloy barrel and plunger tip. The diameter of the die was 0.015 in. and the length was 1 in. Melt stability measurements were generally made at constant temperatures and shear rate (usually at 277 s^{-1}) at regular time intervals up to 25 min. For the purpose of determining melt viscosities, a plot of viscosity vs. shear rate was generated by measuring the viscosities at shear rates of 56, 166, 944, 2388, and 8333 s^{-1}; viscosities at 100 and 1000 s^{-1} were then interpolated.

Compounding and Injection Molding

Polymer samples were compounded with fiber glass fillers ($\frac{1}{8}$ in. chopped strand from Owens Corning) on a Werner Pfleiderer ZSK 28 mm extruder in the temperature range 320–330°C. The glass-filled resins were molded into test specimens on a Boy 30M injection-molding machine with a barrel temperature in the range of 295–320°C. The electrically

heated mold temperature was kept at 100°C in all cases.

Mechanical Property Testing

ASTM procedures were used for the measurement of tensile strength, tensile modulus, and elongation to break (D638); flexural strength and flexural modulus (D790); notched Izod impact strength (D256); and heat-deflection temperature (determined at 264 psi, D648).

Typical Procedure for the Synthesis of *In Situ* Blends of HIQ/LCP

Into a three-neck 2 L glass reactor immersed in a sand bath and equipped with a nitrogen inlet, thermocouple, Vigreux column attached to condenser and receiver, and C-shaped 316 stainless-steel mechanical stirrer were placed (a) 290.1 g (2.1 mol) of HBA, (b) 218.0 g (1.98 mol; 0.05 mol % excess) of HQ, (c) 324.0 g (1.95 mol) of IA, (d) 40.1 g (0.3 mol) of CO (copolyester of HBA/HNA), and 0.063 g (75.5 ppm) of potassium acetate under a constant purge of nitrogen (30–40 cc/min). The reactor was evacuated to approximately 1–2 mbar followed by breaking the vacuum with nitrogen. The vacuum-nitrogen purging process was repeated twice and 637.4 g (6.15 mol, 2.5 mol % excess of 98.5 mol % purity) of acetic anhydride was introduced into the reactor through an addition funnel. The reactor was then heated in stages using a MicRIcon controller from room temperature to 325°C over a period of 6 h.

Acetic acid began distilling when the reactor was at 150°C and about 98% of theoretical amount (687 mL) had evolved when the reactor reached 325°C. The nitrogen purge was then turned off and the reactor was evacuated to about 2 mbar. The torque on the stirrer was monitored and the reaction was terminated when an increase in torque of 50 mV from the initial value was attained. The reactor was cooled and broken to obtain the polymer; yield 713.2 g.

The polymer had an inherent viscosity (IV) of 0.81 dL/g when measured in equal parts by volume of pentafluorophenol/hexafluroisopropanol solvent mixture (0.1% w/v) at 25°C. The melting point (T_m), heat of melting (H_m), glass transition temperature (T_g), crystallization point (T_c), and heat of crystallization (H_c) were found to be 306°C, 6.2 J/g, 128°C, 263°C, and −8.9 J/g, respectively, as determined by differential scanning calorimetry (DSC; 20°C/min heating rate). The melt viscosity of the polymer at 330°C and at shear rates of 100 and 1000 s^{-1} was determined to be 344 and 112 poise, respectively. The polymer melt also exhibited a homogeneous fine texture by light microscopy and the texture was retained after quenching to ambient temperature.

RESULTS AND DISCUSSIONS

Overview

The polymerizations were conducted in 2 or 4 L cylindrical flasks heated in a sand bath reactor. All

Table I Comparative Properties of 30 Wt % Glass-filled *In Situ* Blends

	ASTM Test	Vectra A130	HIQ35	CO–HIQ	MB–HIQ
Composition, CO/HIQ35				5/95	5/95
T_m (°C, solid to nematic)		280	294 and 309	302	299
T_c (°C, nematic to solid)		230	250	262	248
T_g (°C, glass transition)		n.o.	134	132	131
Melt viscosity, poise					
At 100/s		1400	525	611	605
At 1000/s		500	201	205	214
(temp at MV measured, °C)		(300)	(330)	(330)	(330)
Tensile strength (kpsi)	D638	30	15	15.8	18.7
Tensile modulus (Mpsi)	D638	2.4	2	2	1.9
Elongation (%)	D638	2.2	1	1	1.3
Flexural strength (kpsi)	D790	37	21	21	24
Flexural modulus (Mpsi)	D790	2.1	2	1.8	1.9
Notched IZOD impact (ft-lb/in.)	D256	2.8	1.2	1.2	1.3
Heat deflection temp					
264 psi (°C)	D648	230	232	218	231

CO–HIQ, *in situ* blends of CO and HIQ35. MB–HIQ, master *in situ* blends of CO and HIQ35. n.o., not observed.

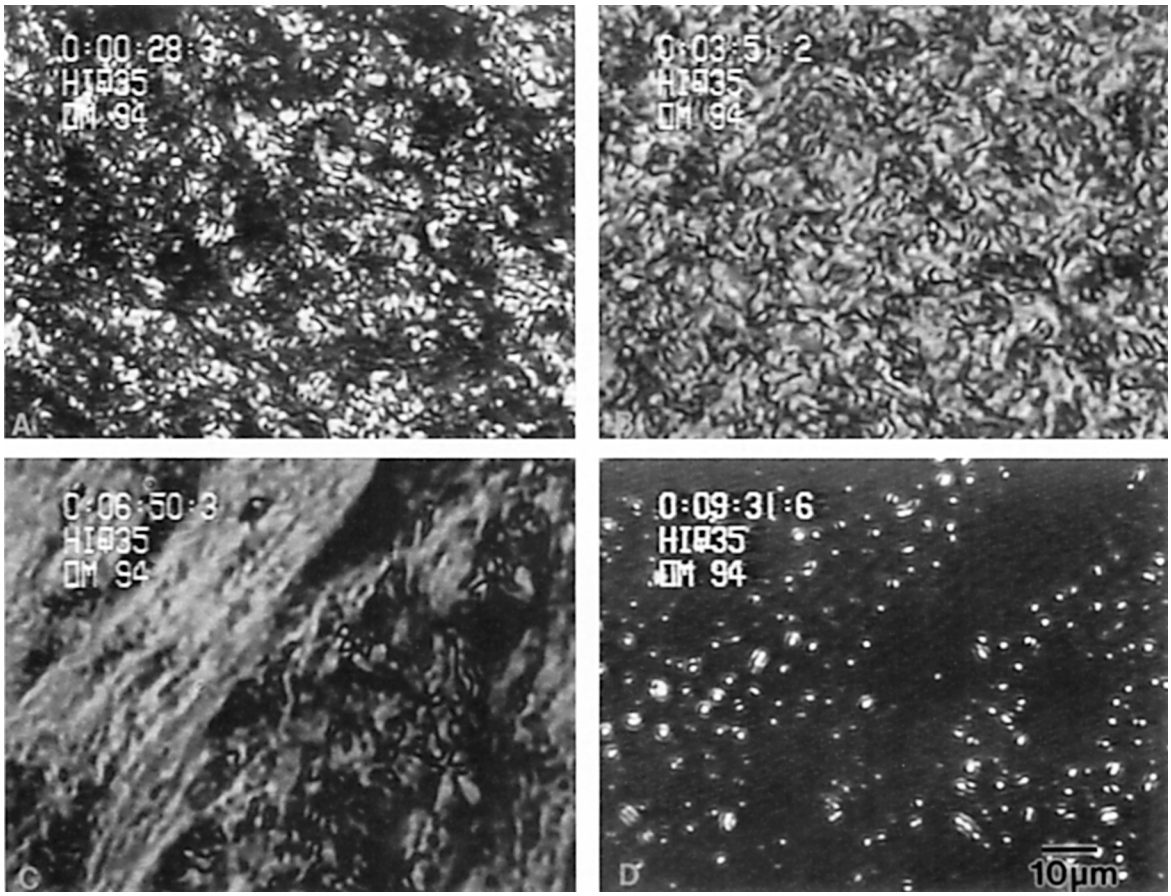

Figure 1 Dynamic polarized light hot-stage micrographs of HIQ35: (A) room temperature; (B) 285°C; (C) 345°C; (D) 395°C (750×).

the condensation reactions reported were carried out by an *in situ* acetylation procedure (ISAP).[13] The hydroxy aromatic compounds were reacted with carboxylic acids in the presence of acetic anhydride, which acted as an acetylating agent as well as a condensating agent. Initially, the acetylation of phenolic groups take place *in situ* to form acetates, which, in turn, react with carboxylic acids to undergo ester interchange to form polyesters. In all cases, potassium acetate was used as the polyesterification catalyst. The LCP, CO, was also introduced into the reactor along with the monomers at the beginning of the polymerization run.

After the polymerization was terminated, the *in situ* blends were cut into pieces and ground into chips for analysis. In a typical experiment, the polymer samples were analyzed for molecular weight by determining the inherent solution viscosity and melt viscosity. The thermal properties were determined by differential scanning calorimetry and the morphology was studied by thermooptical microscopy. The polymer samples were then compounded with glass fibers, generally 30% by weight, and molded into test specimens. The mechanical properties such as tensile, flex, notched Izod, and heat-deflection temperature were measured using these test specimens. In a few selected examples, the polymer samples were spun into fibers and the fiber properties were determined.

Table I summarizes the physical and mechanical properties of some of the *in situ* CO–HIQ blends. Mechanical properties for all compositions listed in Table I were measured according to ASTM procedures. For comparison, the physical properties of HIQ35 and Vectra® A130, a 30% glass-filled CO, are also presented in this table. In general, the *in situ* blends processed at lower temperatures and lower injection pressures than did HIQ35 and their processability appeared to be similar to that of Vectra A130. More importantly, the properties of the *in situ* blends were more reproducible than were those of HIQ35. However, the notched Izod impact strengths for the CO–HIQ compositions were found to be lower than those of Vectra A130 but higher than those of HIQ.

We proposed that the impact properties of CO–

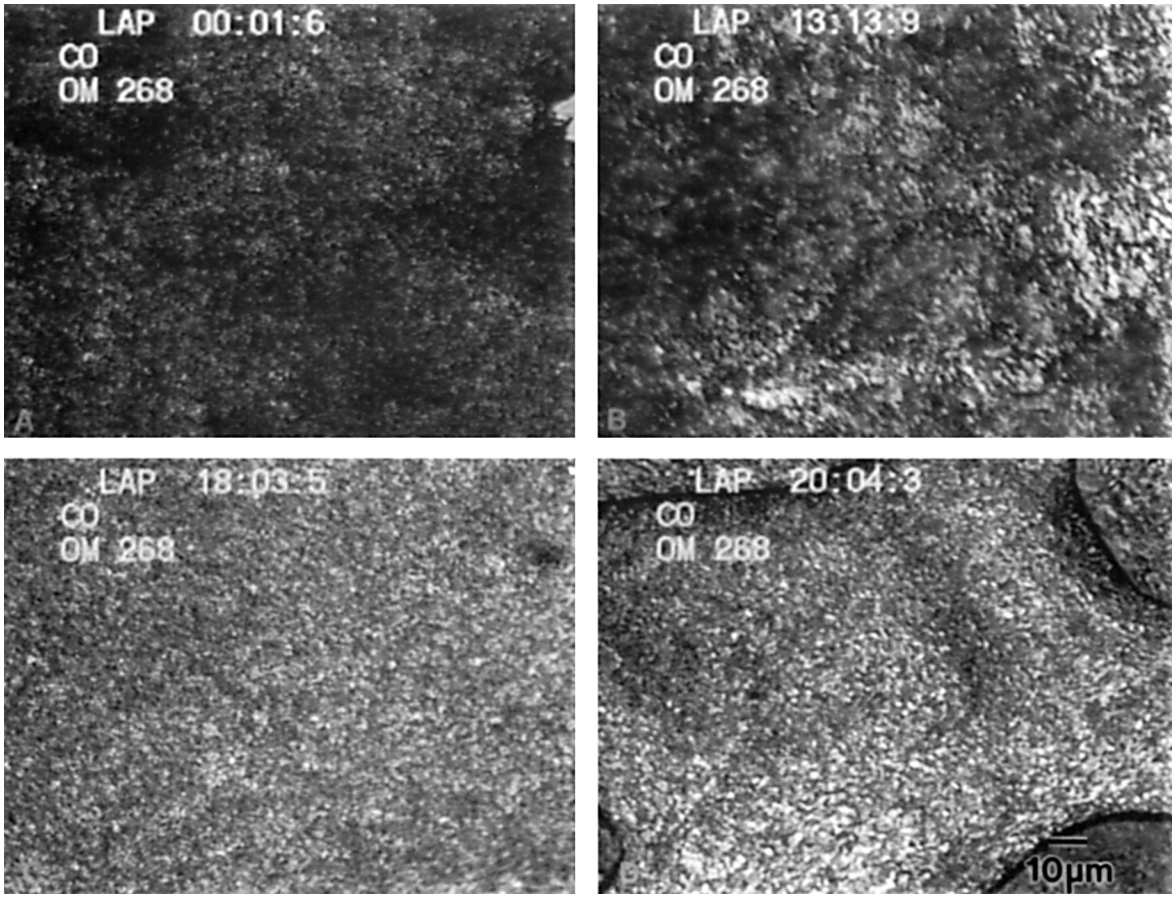

Figure 2 Dynamic polarized light hot-stage micrographs of CO: (A) room temperature; (B) 285°C; (C) 345°C; (D) 395°C (400×).

HIQ could be improved by obtaining an optimal dispersion of CO in CO–HIQ. To further improve the mixing of CO with HIQ, a master batch of 50/50 CO/HIQ35 (MB–HIQ) was prepared, and 10% of the master batch was added to the polymerizing HIQ monomers; the resulting MB–HIQ 10/90 still contains 5 mol % CO. As shown in Table I, the tensile and flexural strength and the heat-deflection temperature for MB–HIQs are improved in comparison to CO–HIQ and marginal increases in impact strength and elongation were observed. The morphologies of these samples were also examined by thermooptical microscopy, which confirmed that the master blending approach provides a means for obtaining improved dispersion of CO in an HIQ matrix (Fig. 3).

Characterization by Light Microscopy

Light microscopy served as a most useful tool in characterizing the morphology of *in situ* blends.[14] Several different methods were used in these characterizations. A quick screening protocol was developed to look at the morphology of fiber samples by polarized light microscopy (PLM). The fibers were generally spun at 340–350°C, and, therefore, if the starting *in situ* blend was biphasic, the fiber formation would clearly lead to phase separation, which can be readily detected by PLM. If fiber samples exhibited reasonably homogeneous morphologies, then those *in situ* blend samples in the form of pellet, chip, or molded part were examined more thoroughly by dynamic polarized light hot-stage microscopic experiments by heating the samples to 400°C followed by rapid quenching.

The light microscopy studies confirmed that the *in situ* polymerization of HIQ in the presence of an LCP offers two unique advantages:

1. The *in situ* process broadens the anisotropic melt phase and processable range of HIQ35 from 320–350°C to about 280–380°C, even in the presence of small amounts of preformed LCP (e.g., 1–2 mol %).

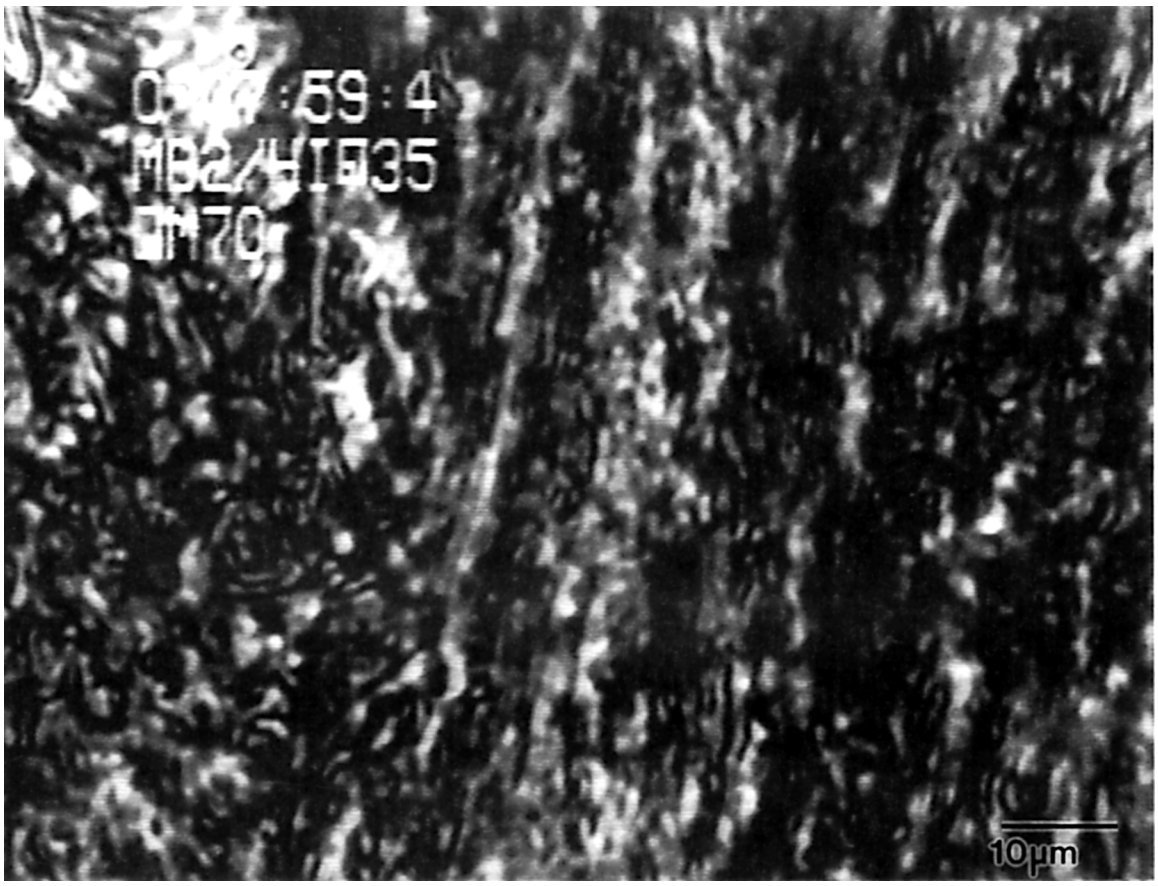

Figure 3 Dynamic polarized light hot-stage micrograph of MB2–HIQ35 *in situ* blend at 345°C (1500×).

2. It reduces the biphasic nature of HIQ35 by reducing the size of the crystalline structure formed due to IA/HQ units.[3(a)]

A few representative light micrographs are shown in Figures 1–6. All the polymer samples were as-synthesized in the chip form. In Figures 1 and 2, the morphology of the samples are shown at four different temperatures: (A) at room temperature; (B) at 285°C; (C) at 345°C; and (D) at 395°C. Figures 3–6 show the morphologies of the samples only at 345°C, the region of interest wherein substantial changes in morphology occurs for HIQ35 (HBA/IA/HQ, 35/32.5/32.5). Therefore, it is of interest to compare the morphology of the blends at this temperature with that of HIQ35 at this temperature.

The light micrographs shown in Figure 1(A)–(D) illustrate typical sections of HIQ35. Coarse crystalline and finer liquid crystalline domains are apparent in the temperature range 285°C [Fig. 1(B)] to 345°C [Fig. 1(C)]. At 345°C, liquid crystalline domains are present in an isotropic melt. At 395°C [Fig. 1(D)], the melt becomes mostly isotropic and is completely isotropic at 410°C. For comparison, Figure 2 illustrates the thermooptical behavior of CO. Uniform liquid crystalline domains are apparent over the entire 285–395°C temperature range [Fig. 2(B), (C), and (D)], and it is clearly evident that the morphology of CO is invariant with the temperature.

Figures 3 and 4 are of MB–HIQ35 (master *in situ* blends of CO with HIQ35) that contained, respectively, 1 and 5 mol % of CO in HIQ35. These *in situ* blends were made by the master blending technique. It is clear from these micrographs that the *in situ* blending of CO with HIQ35 has refined the crystalline texture of the latter. The coarser crystalline regions seen in Figure 1(C) are substantially reduced in Figure 3 and much more so in Figure 4. A finer microstructure than illustrated for HIQ in Figure 1 is clearly evident at temperatures around 345°C, as shown in Figures 3 and 4. It is also interesting to

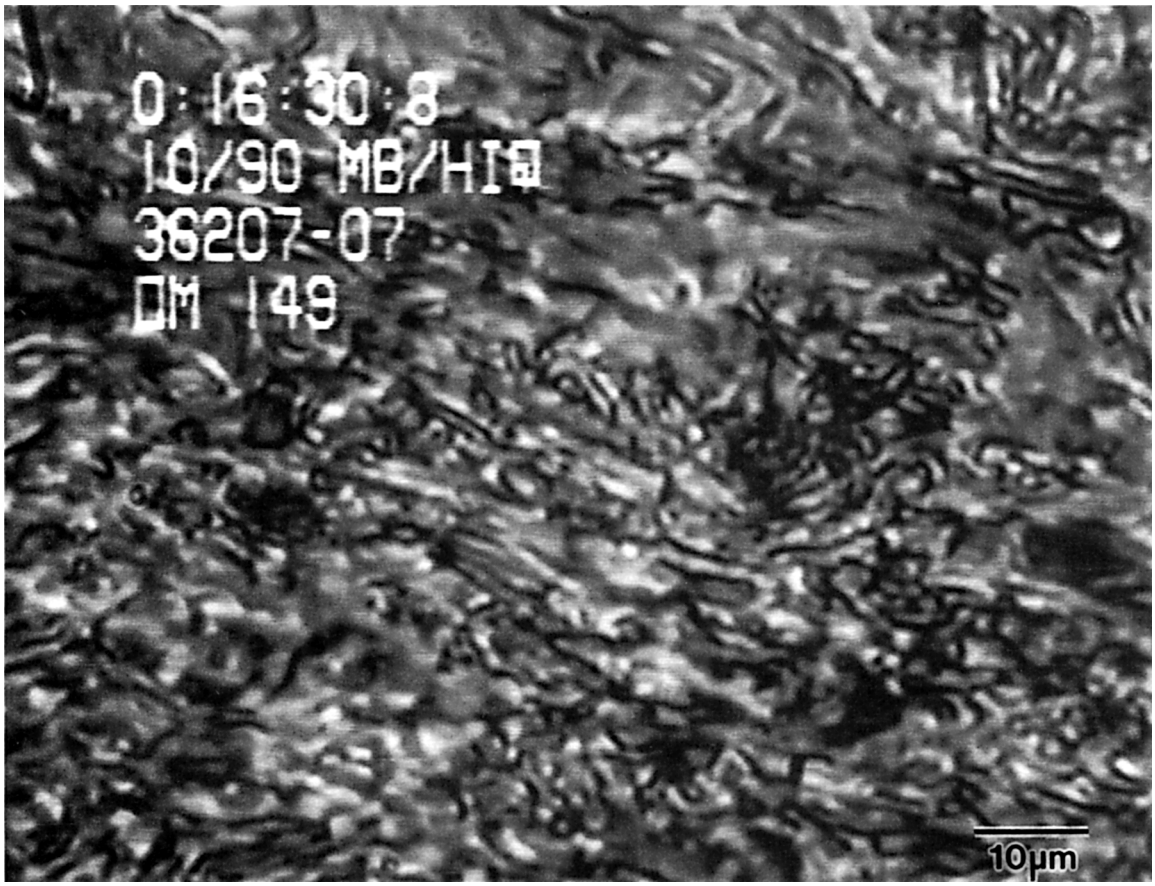

Figure 4 Dynamic polarized light hot-stage micrograph of MB10–HIQ35 *in situ* blend at 345°C (1500×).

note that the microstructure is more refined in Figure 4 than in Figure 3. Furthermore, the isotropic transition is shifted to above 395°C in these *in situ* blends.

In addition, the finer nematic textures seen in Figures 3 and 4 of the *in situ* blends resemble CO and, thus, demonstrate that the *in situ* blending approach offers an opportunity to change the morphology of a major component, such as HIQ, when blended with a suitable minor component such as CO. Although a CO–HIQ of similar composition, 5 : 95 molar ratio of CO : HIQ35, exhibited a finer texture than that of HIQ35, it has a coarser melt morphology than that of MB–HIQ. Thus, the master blending approach results in further refinement of HIQ morphology. It was also confirmed that at higher than 5 mol % of CO the morphology of the CO phase began to coarsen, and at 15 mol % of CO, phase separation was apparent.

The morphologies of *in situ* blends and physical blends of HIQ35 with CO were also compared. The light micrograph shown in Figure 5 illustrates typical sections of a 10 : 90 CO : HIQ35 physical blend at 345°C. It is apparent that it exhibits larger nematic domains and a coarser lamellar-type structure, which is closer to that of HIQ35 at about 345°C [i.e., Fig. 1(C) vs. Fig. 5]. The coarser lamellar-type texture begins to flow at this temperature (Fig. 5) and turns isotropic around 395°C as observed in the case of HIQ35. However, the addition of 10% CO results in a significant refinement of the liquid crystalline melt morphology of HIQ35, even though the morphology of the physical blend is not as refined as that of the *in situ* blends. It should be noted further that the physical blend in Figure 5 contained 10 mol % CO, whereas the *in situ* blend in Figure 4 contained only 5 mol % CO. In spite of lower levels of CO, the *in situ* blend (Fig. 4) featured a more homogeneous morphology than that of the physical blend (Fig. 5).

For comparison, Figure 6 illustrates the light micrograph of a copolyester, COHI (HBA/HNA/HQ/

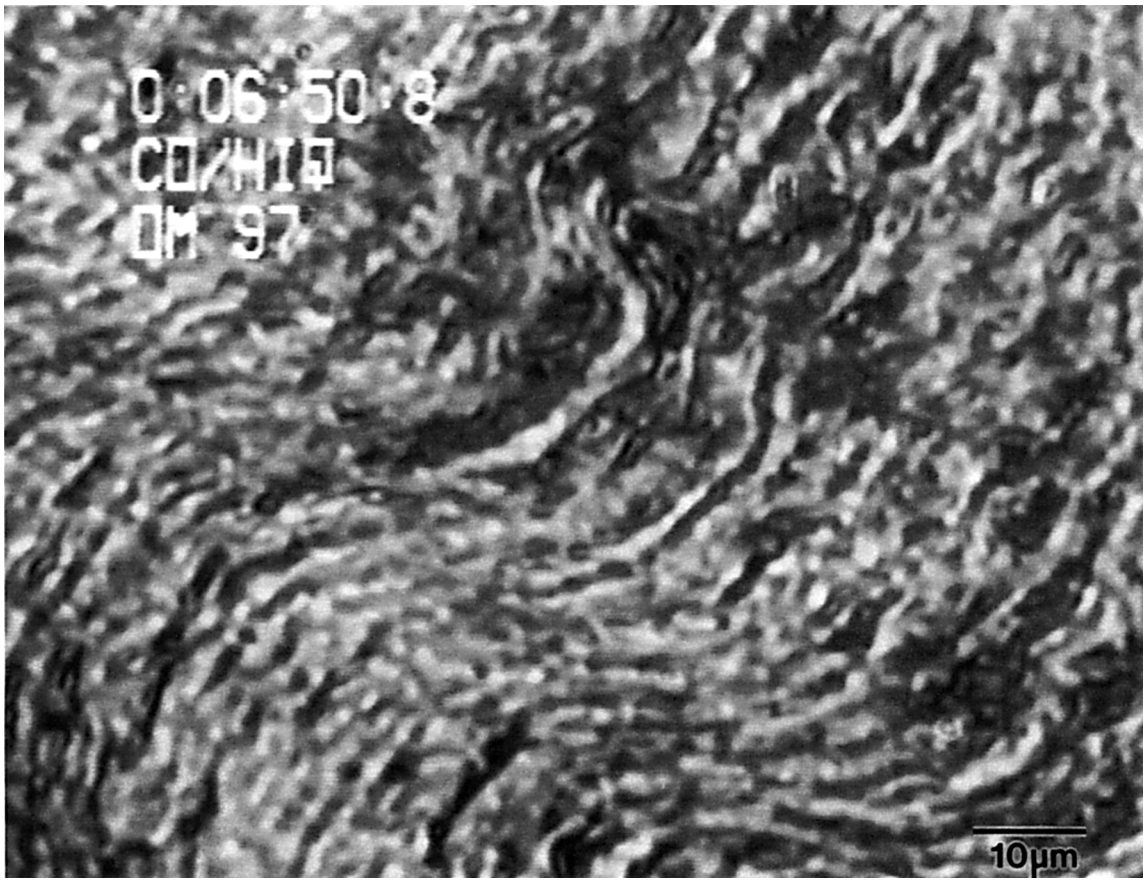

Figure 5 Dynamic polarized light hot-stage micrograph of CO10 : HIQ35 physical blend at 345°C (1500×).

IA, 38.5/2.5/29.5/29.5), which had the same chemical composition as that of CO10 : HIQ35. It is clearly apparent from Figure 6 that COHI exhibits an entirely different morphology than that of either an *in situ* or a physical blend of CO–HIQ, thus demonstrating that the *in situ* technique provides a unique approach to modify the morphology of HIQ35.

NMR Analysis

The light microscopy studies suggest that *in situ* blending offers a method by which a more intimate mix of CO in an HIQ matrix can be achieved than by mere physical blending. This may occur by chemical interaction, i.e., transesterification between CO and HIQ during *in situ* polymerization. Thus, it was decided to examine the *in situ* CO–HIQ blends by ^{1}H-NMR. For this study, a 50 : 50 master *in situ* blend of CO and HIQ35 was used. The ^{1}H-NMR of this sample was compared with that of CO and HIQ35 in order to determine if there was any transesterification between CO and HIQ. Since LCPs are not very soluble in most solvents and only 1–2 wt % of CO–HIQ can be dissolved in pentafluorophenol-*d* (PFP-*d*), only the master *in situ* blend was chosen for this study. A copolyester, COHI (HBA/HNA/HQ/IA, 54/13.5/16.25/16.25), which had the same chemical composition as that of the master batch, was also made for this study. This polymer would be expected to have a statistical distribution of monomers in its random polymer backbone and thus would serve as a direct comparison with the master batch to determine the extent of transesterification.

The ^{1}H-NMR studies show that transesterification between CO and HIQ does take place during *in situ* polymerization. The degree of transesterification, however, could not be estimated from ^{1}H-NMR due to overlapping signals in the region of interest. The transesterification between CO and HIQ was monitored by signals due to triad sequences. The

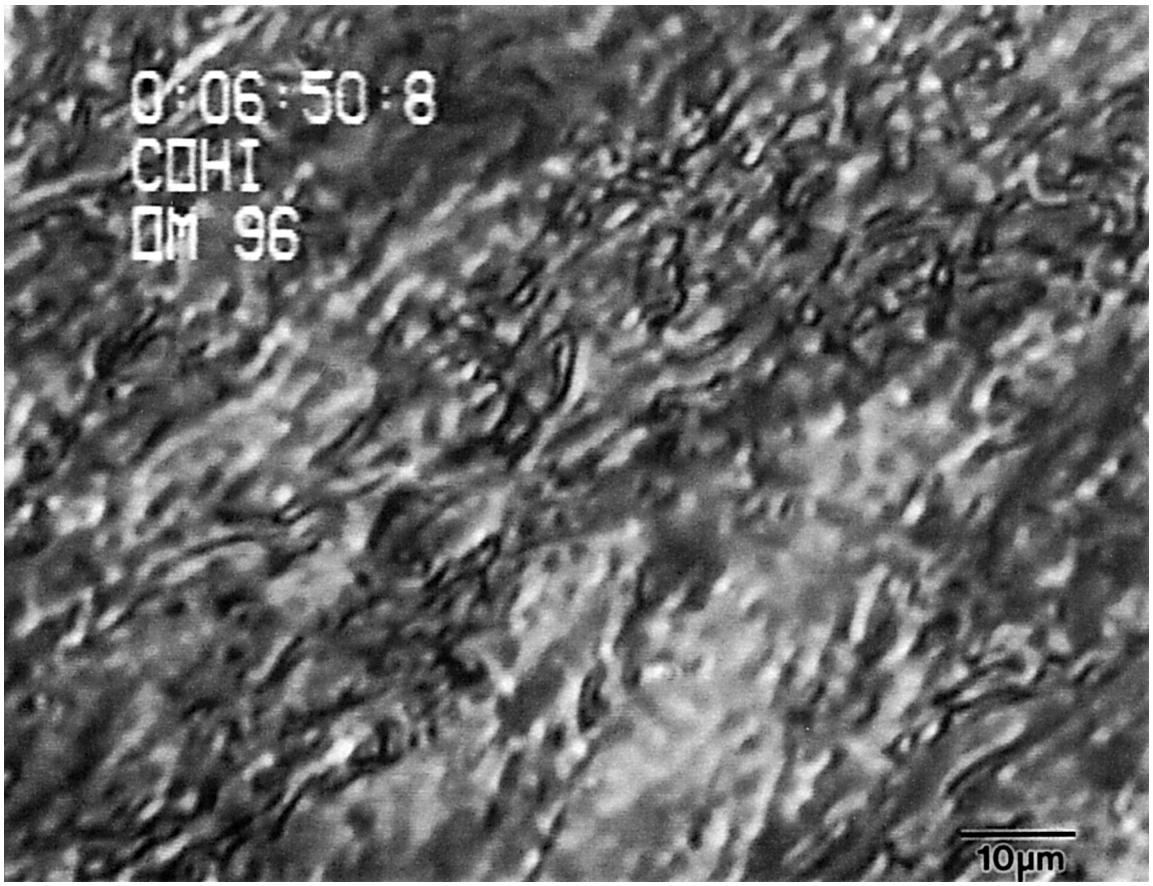

Figure 6 Dynamic polarized light hot-stage micrograph of COHI at 345°C (1500×).

signal due to the proton of the isophthalic acid (i.e., 2-H on the ring) served as an indicator for this purpose. Figure 7 shows the portion of interest of the ^{1}H-NMR spectra of (a) COHI, (b) a 50 : 50 master *in situ* blend of CO with HIQ35, and (c) HIQ35. The spectrum in Figure 7(b) indicates that there are at least five signals due to the isophthalic acid proton around 9.28 ppm, which suggests that at least five different triad sequences are formed with IA. The ^{1}H-NMR spectrum of HIQ35 [Fig. 7(c)] shows three signals for this proton due to the three possible triad sequences, namely, HBA–IA–HBA, HBA–IA–HQ, and HQ–IA–HQ. Figure 7(a) exhibits a similar spectrum as that of the master batch in Figure 7(b) with the exception that much broader peaks for the isophthalic acid proton were observed. The additional peaks are due to the triad sequences such as HBA–IA–HNA, HQ–IA–HNA, and HNA–IA–HNA. This clearly suggests that transesterification between CO and HIQ has taken place in the master batch. However, quantification of the degree of transesterification could not be made from this study since the peak resolution was poor and proper assignment of the signals due to the various sequences was not done.

Characterization of CO–HIQ *In Situ* Blends by Melt Rheology

It was stated earlier that HIQ35 exhibits a narrow nematic transition around 290–320°C and a very broad isotropic transition from 320 to 395°C, as observed by thermooptical microscopic studies. In fact, this phenomenon results in an anomalous positive temperature coefficient of viscosity in the measured temperature range of 340–360°C (viscosity increasing with shear rate and temperature, see Fig. 8).[15] This unusual variation in rheological behavior of HIQ35 leads to problems with reproducibility of the polymer during its preparation as well as during processing. An attempt has been made to broaden the nematic transition by applying high pressures.[16] In the present study, it was determined that the nematic transition was broadened by *in situ* polymerization.

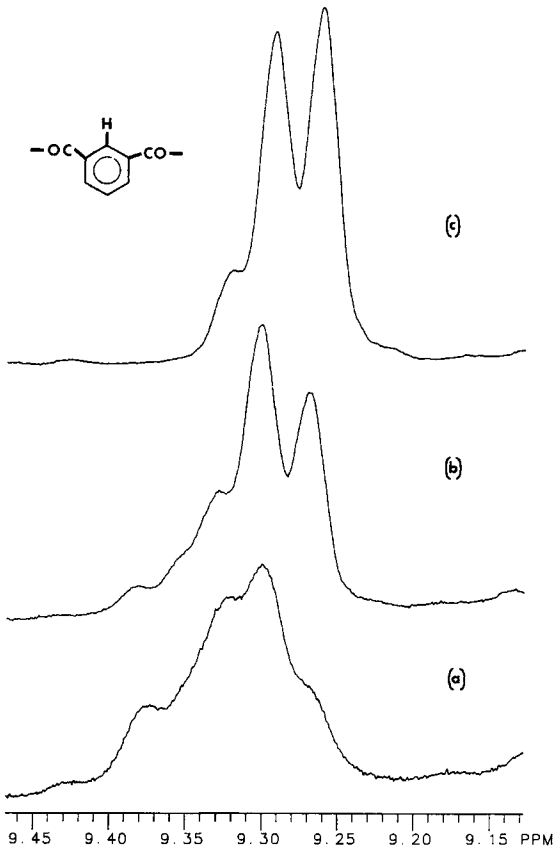

Figure 7 Downfield portions of ^{1}H-NMR spectra of (a) COHI, (b) 50 : 50 master *in situ* blend of CO with HIQ35, and (c) HIQ35.

Figure 8 is a plot of the log of melt viscosity of HIQ35 and two compositions of CO–HIQ vs. inverse temperature. Kiss[15] reported in his studies that HIQ35 became increasingly viscous as temperature is increased and the viscosity increased up to an order of magnitude over a 40° range. In this work, HIQ35 was reexamined along with CO5–HIQ35 (5 mol % CO in HIQ35) and CO10–HIQ35 (10 mol % CO in HIQ35), making measurements at smaller increments (5°) in the 315–355°C range. The resulting curve for HIQ35 in Figure 8 shows a narrow flat region (325–340°C) where the viscosity is relatively insensitive to temperature (i.e., nematic region). This is a small "window of processability" in which the behavior of the material may be reliably controlled. Polymerizations completed at temperatures near the end of this window are subject to irreproducibility since relatively small temperature variations can produce large changes in viscosity. The flat regions of the CO–HIQ curves cover a much wider temperature range (in excess of 25°C from 320 to 350°C, see Fig. 8). The viscosities of the CO–HIQs do not appear to increase significantly at higher temperatures and, therefore, wider processing windows are available. Furthermore, the effect of temperature variation during final polymerization is decreased and, thus, the reproducibility of the process is improved. It should also be noted that the higher the level of CO in CO–HIQ the lower the melt viscosity (Fig. 8).

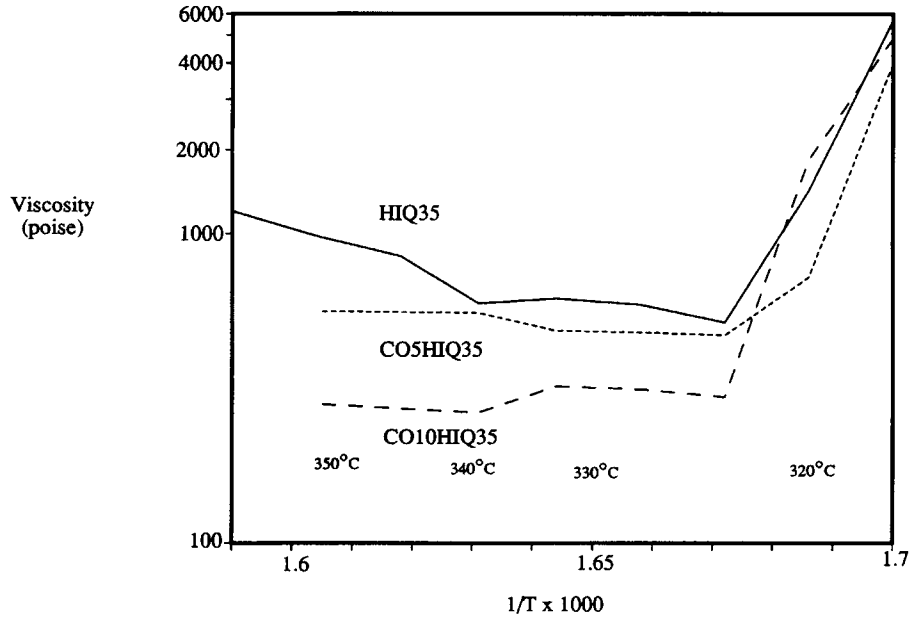

Figure 8 Melt rheology of CO–HIQ *in situ* blends vs. HIQ35 at shear rate of 277 s^{-1} as a function of temperature.

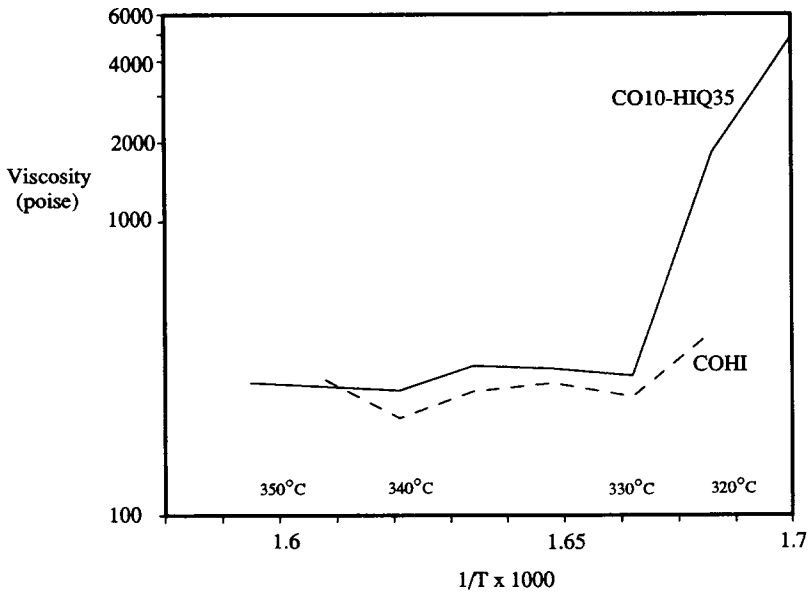

Figure 9 Melt rheology of CO–HIQ *in situ* blends vs. COHI of identical monomer composition at shear rate of 277 s^{-1} as a function of temperature.

Figure 9 compares the viscosity profile of CO10–HIQ35 with a COHI polymer of identical monomer composition (HBA/HNA/HQ/IA, 38.5/2.5/29.5/29.5). The COHI has a generally lower viscosity with a more gradual increase near the melting point and a small increase at higher temperatures. This comparison further confirms that the CO–HIQ is a unique material and not a simple COHI polymer, as also confirmed in the NMR studies.

CONCLUSIONS

This study has demonstrated that the morphology of biphasic liquid crystalline polymers (LCPs) can be altered by *in situ* polymerization of the biphasic polymer in the presence of a fully preformed LCP. The HIQ/LCP polymers made in this fashion have much broader nematic transitions, thus providing a broader processing window and more reproducible mechanical properties. Batch-to-batch variation is also improved. It was also found that master blending further improves the dispersion of the preformed LCP. The *in situ* master blends, in general, feature better properties than the *in situ* blends made in one step. The light microscopic characterizations showed that *in situ* blends feature finer homogeneous morphology than that of HIQ35 and physical blends of identical compositions. The ^{1}H-NMR analysis indicated that some transesterification occurs between HIQ and CO, which may be the reason for differences in morphologies between physical and *in situ* blends of similar compositions as observed by light microscopy. The *in situ* polymerization concept may be extended to the synthesis of various other incompatible blends, thereby improving the compatibility of the blend components and thus more homogeneous blends can be formed. Preliminary work in this area has given some interesting results and details of this work will be published elsewhere.

The authors wish to thank Hoechst Celanese for support of this work. Technical assistance in preparation and characterization of the samples by M. Bylicki, A. Congreve, and V. Provino is gratefully acknowledged. The authors would also like to thank J. Gaede for the NMR studies and T. Bruno for the thermooptical studies. Last but not the least, constructive comments in the preparation of this manuscript by our colleagues, Drs. M. Borzo and C. Lee, are highly appreciated.

REFERENCES

1. S. G. Cottis, J. Economy, and B. E. Nowak, U.S. Pat. 3,637,595 (Jan. 25, 1972) (to The Carborundum Co.).
2. H.-B. Tsai, C. Lee, N.-S. Chang, M.-S. Chen, and S.-J. Chang, *J. Appl. Polym. Sci.*, **40,** 1499 (1990), and references cited therein.
3. (a) A. B. Erdemir, D. J. Johnson, and J. G. Tomka, *Polymer,* **27,** 441 (1986); (b) D. J. Johnson, I. Karacan, and J. G. Tomka, *Polymer,* **32,** 2312 (1991), and references cited therein.
4. A. J. East, Hoechst Celanese Internal Report.

5. W. A. MacDonald and T. G. Ryan, U.S. Pat. 4,868,278 (Sep. 19, 1989) (to Imperial Chemical Industries).
6. R. K. Siemionko, U.S. Pat. 4,370,466 (Jan. 25, 1983) (to E. I. Du Pont de Nemours & Co.).
7. (a) R. Layton, J. W. Cleary, P. J. Huspeni, P. D. Frayer, and M. Matzner, U.S. Pat. 5,079,289 (Jan. 7, 1992); (b) B. A. Stern, M. Matzner, and R. Layton, U.S. Pat. 5,089,594 (Feb. 18, 1992); (c) B. A. Stern, M. Matzner, R. Layton, P. Huspeni, P. D. Frayer, and J. W. Cleary, PCT WO 90/04003 (Apr. 19, 1990); (d) P. Huspeni, B. A. Stern, P. D. Frayer, R. Layton, and M. Matzner, U.S. Pat. 5,066,767 (Nov. 19, 1991); (e) P. Huspeni, R. Layton, and P. D. Frayer, U.S. Pat. 5,091,464 (Feb. 25, 1992) (all to Amoco Corp.).
8. M. Matzner and D. Papuga, PCT WO 88/00605 (Jan. 28, 1988); Eur. Pat. Spec. 0,214,612 (Nov. 30, 1988) (to Amoco Corp.).
9. H. Sugimoto and M. Hanabata, U.S. Pat. 4,414,365 (Nov. 8, 1983) (to Sumitomo Chemical Co.).
10. P. R. Ginnings, U.S. Pat. 4,778,858 (Oct. 18, 1988) (to The Goodyear Tire & Rubber Co.).
11. F. N. Cogswell, B. P. Griffin, and J. B. Rose, U.S. Pat. 4,438,236 (Mar. 20, 1984) (to Imperial Chemical Industries).
12. For a detailed description of various examples, see L. F. Charbonneau, B. Gupta, H. C. Linstid, L. C. Sawyer, and J. P. Shepherd, World Pat. 9,304,127 A1 (Mar. 4, 1993) (to Hoechst Celanese Corp.).
13. (a) L. F. Charbonneau, U.S. Pat. 4,429,105 (Jan. 31, 1984) (to Hoechst Celanese Corp.); (b) for a general review on esterification, see E. G. Zey, in *Kirk Othmer's Encyclopedia of Chemical Technology,* 3rd ed., Wiley, New York, 1980, Vol. 9.
14. L. C. Sawyer and D. T. Grubb, *Polymer Microscopy,* Chapman and Hill, London, 1987.
15. G. Kiss, *J. Rheol. (N.Y.),* **30,** 585 (1986), and references cited therein.
16. B. S. Hsiao, M. T. Shaw, and E. T. Samulski, *Macromolecules,* **21,** 543 (1988).

Received August 11, 1993
Accepted December 13, 1993